A spectroscopic comparison between several high-symmetry $S=10$ Mn_{12} single-molecule magnets

S. Hill,[a] N. Anderson, A. Wilson, and S. Takahashi
Department of Physics, University of Florida, Gainesville, Florida 32611

N. E. Chakov and M. Murugesu
Department of Chemistry, University of Florida, Gainesville, Florida 32611

J. M. North and N. S. Dalal
Department of Chemistry and Biochemistry, Florida State University, Tallahassee, Florida 32310

G. Christou
Department of Chemistry, University of Florida, Gainesville, Florida 32611

(Presented on 10 November 2004; published online 16 May 2005)

We report angle-dependent high-field electron-paramagnetic-resonance data collected for single-crystal samples of Mn_{12}−Ac. The spectra reveal fine structures associated with various Mn_{12} species corresponding to different disordered local environments. Each of the fine structures exhibits a distinct dependence on the field orientation, thereby highlighting the discrete nature of the disorder. We compare these data with the spectra obtained for two recently discovered analogs of Mn_{12}−Ac, differing only in their ligand and solvent molecules. None of the fine structures seen for Mn_{12}−Ac are found for the recently discovered Mn_{12} complexes, thus confirming that the solvent significantly influences the magnetization dynamics in Mn_{12}−Ac.
 [DOI: 10.1063/1.1851433]

$[Mn_{12}O_{12}(O_2CCH_3)_{16}(H_2O)_4]\cdot 2CH_3COOH\cdot 4H_2O$ (Mn_{12}−Ac) has become the most widely studied single-molecule magnet (SMM) due to its giant spin ($S=10$) ground state and its high symmetry (S_4).[1] These factors result in the largest blocking temperature ($T_B\sim 3$ K) against magnetization relaxation of any known SMM. In spite of over ten years of research, a clear picture has only recently emerged concerning the symmetry breaking responsible for the quantum magnetization tunneling (QMT) in Mn_{12}−Ac.[2–6] Several studies have shown that disorder associated with the acetic acid solvent leads to discrete local environments, resulting in a significant fraction of the molecules ($>50\%$) possessing twofold symmetry with a rhombic crystal-field term E on the order of 0.01 cm^{-1} (or $E/D\sim 0.02$, where D is the uniaxial crystal-field parameter).

Here, we compare high-field/frequency electron-paramagnetic-resonance (HFEPR) data obtained for the usual Mn_{12}−Ac with two recently discovered variants, both of which possess the same S_4 site symmetry. The newer compounds are $[Mn_{12}O_{12}(O_2CCH_2Br)_{16}(H_2O)_4]\cdot 4CH_2Cl_2$ (Refs. 7 and 8) and $[Mn_{12}O_{12}(O_2CCH_2Bu^t)_{16}(H_2O)_4]\cdot CH_3OH$, abbreviated Mn_{12}−BrAc and Mn_{12}−*t*BuAc, respectively. The motivation for the present undertaking is to investigate the influence of the solvent structure on the properties of the $Mn_{12}O_{12}$ core, which is virtually identical for the three complexes. As our recent studies have shown,[3,5,6] angle-dependent single-crystal HFEPR measurements provide precise details concerning the distributions of local environments in a crystal of SMMs, e.g., we have been able to characterize the nature of the rhombicity of the lower-symmetry Mn_{12}−Ac variants brought about by solvent disorder,[3] as well as showing that the magnetic axes are tilted with respect to the global easy axis of the crystal.[5]

Single-crystal HFEPR measurements were carried out using a millimeter-wave-vector network analyzer (MVNA) in combination with a cavity perturbation technique which we have described elsewhere.[9] In order to enable *in situ* two-axis rotation of the sample relative to the applied magnetic field, we employed a split-pair magnet with a 7 T horizontal field and a vertical access, together with a unique cylindrical cavity in which the sample may be rotated about a second orthogonal axis (this cavity is described in Ref. 10). Single-axis rotation measurements were also performed in a 17 T axial superconducting magnet using the rotating cavity.[10] In both setups, the sample temperature was controlled using helium flow cryostats and calibrated Cernox™ resistance sensors. Mn_{12}−Ac samples were prepared according to the usual methods.[11] Mn_{12}−BrAc crystals were prepared by a ligand substitution procedure involving the treatment of Mn_{12}−Ac with an excess of $BrCH_2CO_2H$.[7,8] Mn_{12}−*t*BuAc crystals were prepared via a method similar to the one in Ref. 12, albeit that CH_3OH solvent was used in the present case, thereby yielding the high-symmetry complex (full details will be presented elsewhere[13]). All samples were handled identically with a view to avoiding solvent loss from the structure; the needle-shaped single crystals ($\sim 1.5\times 0.4\times 0.4$ mm^3) were removed directly from their mother liquor and protected with grease before cooling under 1 atm of helium gas.

Figure 1 displays the HFEPR spectra obtained for the three complexes with the magnetic field applied precisely in the hard plane ($\pm 0.1°$); the frequency is approximately

[a]Electronic mail: hill@phys.ufl.edu

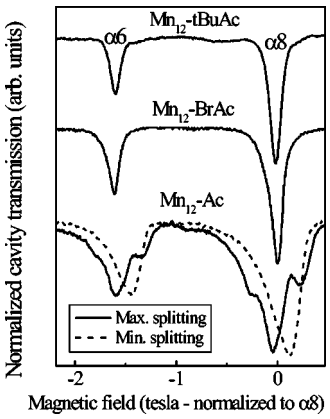

FIG. 1. HFEPR spectra obtained for the three complexes (see labels) with the magnetic field applied precisely in the hard plane (±0.1°); the frequency is approximately 51.5 GHz in each case (±0.3 GHz), and the temperature is 15 K. The magnetic-field axis is referenced to the average position of the $\alpha 8$ peak (see Ref. 5 for explanation of labeling).

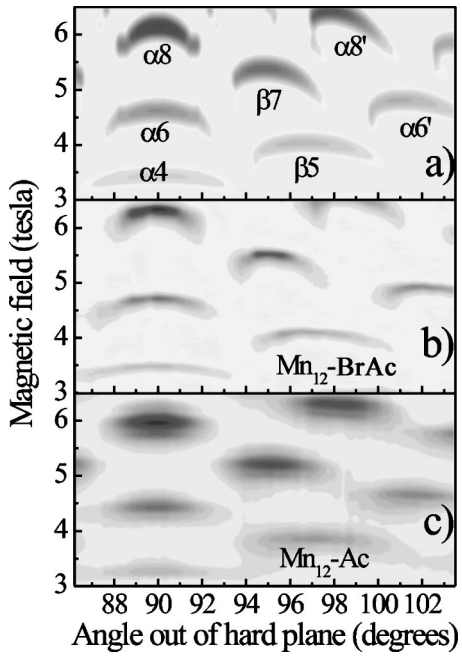

FIG. 2. Gray-scale contour plots of EPR absorption intensity (dark-shaded regions) vs magnetic-field orientation relative to the easy axis of the sample; the temperature is 15 K and the frequency is 51.5 GHz in each case. (a) shows simulated spectra for a spin $S=10$ system with the $Mn_{12}-BrAc$ Hamiltonian parameters (see text), and no disorder, (b) shows actual experimental data for the $Mn_{12}-BrAc$ complex, and (c) shows experimental data for $Mn_{12}-Ac$. The field rotation plane was chosen so as to maximize the splittings of the shoulders away from the main peaks (solid curve in Fig. 1), corresponding to the hard/medium directions of the disorder-induced rhombic tensor.

51.5 GHz in each case (±0.3 GHz), and the temperature is 15 K. The dips in transmission through the cavity correspond to EPR. In order to correct for slight frequency differences between the measurements, as well as differences in the orientation of the field within the hard plane for the $Mn_{12}-Ac$ sample, the magnetic-field axis is referenced to the average position of the $\alpha 8$ peak (see Ref. 5 for explanation of labeling), which occurs at about 6.1 T at 51.5 GHz. It is immediately apparent that the EPR peaks for the BrAc and *t*BuAc complexes are considerably sharper than those obtained for the Ac complex. Furthermore, the $Mn_{12}-Ac$ resonances reveal clear fine structures (high- and low-field shoulders) which vary with the field orientation within the hard plane (dashed and solid curves). The behavior of these fine structures, which are caused by the different local solvent environments (E strain), has been discussed in great detail in our previous publications.[3,5,6] We note that studies of the $Mn_{12}-BrAc$ and $Mn_{12}-t$BuAc complexes for different field orientations within the hard plane indicate no evidence for these fine structures.

The key result in this paper is the absence of the EPR fine structures in the two Mn_{12} complexes, thus suggesting that the QMT in $Mn_{12}-BrAc$ and $Mn_{12}-t$BuAc may reflect the intrinsic S_4 symmetry of the Mn_{12} molecule. This contrasts the situation for $Mn_{12}-Ac$ where the QMT is significantly influenced by the hydrogen bonding to surrounding disordered acetic acid solvent molecules. The crystal-field parameters for the BrAc complex are almost identical to those of $Mn_{12}-Ac$ (see Ref. 8). Comprehensive angle-dependent HFEPR studies for the *t*BuAc complex indicate a slightly larger D value of $0.462(2)\ cm^{-1}$; the remaining parameters are $B_4^0=2.5(2)\times10^{-5}\ cm^{-1}$, $B_4^4=4.3(5)\times10^{-5}\ cm^{-1}$, $g_z=2.00(2)$, and $g_x=g_y=1.94(2)$.

A further illustration of the differences between $Mn_{12}-Ac$ and the BrAc and *t*BuAc complexes is illustrated in Fig. 2. The top panel (a) displays simulations of the out-of-plane angle dependence of the HFEPR absorption intensity for a spin $S=10$ system with the $Mn_{12}-BrAc$ Hamiltonian parameters, and no disorder; the angle corresponds to the field orientation relative to the easy axis of the crystal, and the darker regions represent EPR absorption (see also Fig. 1). In Fig. 2(b), actual experimental data are displayed for the $Mn_{12}-BrAc$ complex. The data are in very good agreement with the simulations, i.e., the EPR intensity alternates between the α and β transitions as the field is tilted away from the hard plane, with clear gaps in between (see Ref. 5 for a detailed explanation for this behavior). Furthermore, most of the curvature associated with the bands of absorption is reproduced in the experiments, which is an indication that the molecular easy axes are very well aligned ($<\pm0.5°$); similar results are found for $Mn_{12}-t$BuAc. In contrast, the regions of absorption for $Mn_{12}-Ac$ [Fig. 2(c)] are considerably broader, displaying clear streaks on the high- and low-field sides of the main absorption bands. These streaks correspond to the shoulders observed in Fig. 1 (solid curve). Also notable is the fact that each of the absorption bands for $Mn_{12}-Ac$ is extremely flat, and they extend over angle ranges exceeding those in the simulations [Fig. 2(a)], as evidenced by the overlapping α and β EPR intensities. We note that the fine structures seen for $Mn_{12}-Ac$ are completely reproducible. Indeed, the data in Fig. 2 were obtained for samples grown by a different group than those presented in Refs. 3, 5, and 6.

As we have already documented,[5] the out-of-plane angle dependence of the EPR spectra for $Mn_{12}-Ac$ can be understood as resulting from significant easy-axis tilting. To illustrate this point, Fig. 3 displays a simulation of the $Mn_{12}-Ac$ data which consists of a superposition of spectra corresponding to the three main species in Cornia's solvent disorder

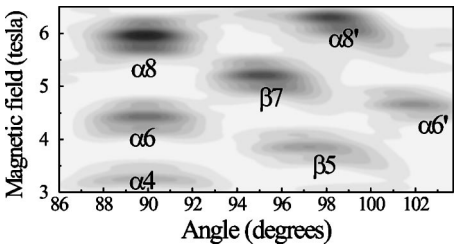

FIG. 3. Gray-scale contour simulations of the data in Fig. 2(c). See main text for an explanation of these simulations.

model. We assume that 50% of the molecules possess no E term, so that they contribute to the strongest central portions of the EPR absorption bands. Of the remaining 50%, half possess an E value of $+0.014(2)$ cm^{-1}, and the other half an E value of -0.014 cm^{-1} (a change in the sign of E is equivalent to a 90° rotation of the hard and medium directions). These molecules contribute to the high- and low-field shoulders on the $Mn_{12}-Ac$ EPR peaks (see Fig. 1) when the field is applied along either the hard or medium magnetic axes induced by the disordered solvent molecules. The flattening of the absorption bands is then reproduced by convoluting the individual contributions to the spectrum with a Gaussian function, $\exp[-(\theta-90°)^2/2\sigma^2]$, where θ is the orientation of the field relative to the global easy axis of the crystal. The full width at half maximum (FWHM) ($w \sim 2.35\sigma$) of the distribution used in Fig. 3 is 2.6°. Overall agreement with the experimental spectrum in Fig. 2(c) is very good. The FWHM of the distribution is found to vary for different planes of rotation (to be published elsewhere[14]), confirming our recent assertion that the easy-axis tilting is confined to orthogonal planes defined by the disorder-induced rhombic (E) zero-field tensor.

The above E value [$\pm 0.014(2)$ cm^{-1}], which was determined from separate in-plane angle-dependent measurements for $Mn_{12}-Ac$ (to be published elsewhere[14]), is larger than the value of $0.008(2)$ cm^{-1} reported in Refs. 3–5. We note that the crystal used in the present study was transferred directly from the mother liquor to the experimental cryostat, whereas those used in earlier experiments were removed from the mother liquor long (up to two years) before performing the EPR measurements. We therefore speculate that the E strain may be reduced in older samples, possibly due to solvent loss. Most notably, the low-field shoulder seen in Fig. 1 for $Mn_{12}-Ac$ is not resolved from the main peak in the earlier experiments, even though we suggested that it should exist.[3–5]

In summary, we compare the HFEPR data for $Mn_{12}-Ac$ with the spectra obtained for two recently discovered Mn_{12} analogs, differing only in their ligand and solvent structures. None of the fine structures seen for $Mn_{12}-Ac$ are found for the recently discovered complexes, thus confirming that the solvent significantly influences the EPR spectra and, therefore, the QMT dynamics in $Mn_{12}-Ac$.

This work was supported by the National Science Foundation (Grant Nos. DMR0103290, DMR0239481, and CHE0414155). One of the authors (S.H.) is a Cottrell scholar of the Research Corporation.

[1] D. Gatteschi and R. Sessoli, Angew. Chem. **42**, 268 (2003).
[2] A. Cornia, R. Sessoli, L. Sorace, D. Gatteschi, A. L. Barra, and C. Daiguebonne, Phys. Rev. Lett. **89**, 257201 (2002).
[3] S. Hill, R. S. Edwards, S. I. Jones, J. M. North, and N. S. Dalal, Phys. Rev. Lett. **90**, 217204 (2003).
[4] E. del Barco, A. D. Kent, E. M. Rumberger, D. N. Hendrickson, and G. Christou, Phys. Rev. Lett. **91**, 047203 (2003).
[5] S. Takahashi, R. S. Edwards, J. M. North, S. Hill, and N. S. Dalal, Phys. Rev. B **70**, 094429 (2004).
[6] E. del Barco *et al.*, eprint arXiv/ cond-mat/0404390.
[7] J. An, Z.-D. Chen, X.-X. Zhang, H. G. Raubenheimer, C. Esterhuysen, S. Gao, and G.-X. Xu, J. Chem. Soc. Dalton Trans. **22**, 3352 (2001); H.-L. Tsai, D.-M. Chen, C.-I. Yang, T.-Y. Jwo, C.-S. Wur, G.-H. Lee, and Y. Wang, Inorg. Chem. Commun. **4**, 511 (2001).
[8] K. Petukhov, S. Hill, N. E. Chakov, K. A. Abboud, and G. Christou, Phys. Rev. B **70**, 054426 (2004).
[9] M. Mola, S. Hill, P. Goy, and M. Gross, Rev. Sci. Instrum. **71**, 186 (2000).
[10] S. Takahashi and S. Hill, Rev. Sci. Instrum. **76**, 023114 (2005).
[11] T. Lis, Acta Crystallogr., Sect. B: Struct. Crystallogr. Cryst. Chem. **36**, 2042 (1980).
[12] M. Soler, W. Wernsdorfer, Z. Sun, J. C. Huffman, D. N. Hendrickson, and G. Christou, Chem. Commun. (Cambridge) **2003**, 2672 (2003).
[13] M. Murugesu *et al.* (unpublished).
[14] S. Hill, N. Anderson, A. Wilson, S. Takahashi, N. Chakov, M. North, N. Dalal, and G. Christou, Polyhedron (to be published).